



Ocean Circulation Modeling : The Bay of Bengal

OPB 205 Modélisation de la Circulation Océanique

Anna-Maria RAMMOU Master 1, Océanographie-Physique-Biogéochimique

2012

Contents

| | |
|------------------------|----|
| Résumé-Abstract | 3 |
| Introduction | 4 |
| Materials and Methods | 4 |
| Results and Discussion | 11 |
| Conclusion | 18 |
| Bibliography | 19 |
| Annex | 21 |

Résumé

La circulation dans la Baie du Bengal est très complexe à cause du régime de vent qui change deux fois dans l'année. Dans cette étude, la simulation de la circulation était réalisée par le modèle ROMS qui est un modèle régional, tridimensionnel, de surface libre et qui suit la topographie. La climatologie était obtenue par ICOADS(05). La zone équatoriale au Nord et la Mer d'Andaman ont été exclus à cause de la dimension de la grille choisie. En plus, la résolution choisie étant faible, il n'a pas été possible de simuler le flux à travers détroit de Sri Lanka et de l'Inde. Pour ces raisons, les résultats de notre simulation ne sont pas totalement en accord avec les autres études qui sont mentionnées ici. Néanmoins, le modèle a simulé le courant de la frontière ouest du bassin (WBC) pendant le printemps et le courant le long de la côte est Indienne (EICC). Les changement saisonniers de la direction de la circulation grâce aux moussons ont été aussi simulés.

Mots clés : Baie du Bengal, Modélisation de la circulation, ROMS, moussons, WBC, EICC

Abstract

The complicated current pattern of the Bay of Bengal is simulated in this present study by a regional, three-dimensional, free-surface, terrain-following numerical model (ROMS) forced by the ICOADS(05) winds. The north equatorial zone and the Andaman Sea are excluded from the grid dimensions used in the area of study. Furthermore the low resolution cannot simulate the flow through the straight between Sri Lanka and India. It was assumed that these reasons were responsible for the discrepancies between our results and those of other studies mentioned here. Nevertheless the model was able to detect the Western Boundary Current (WBC) that intensifies during spring and the southward East India Coastal Current (EICC) in autumn. The seasonal changes depending on the northeast or southwest monsoon were also simulated.

Keys Words : Bay of Bengal, Circulation Modeling, ROMS, monsoons, WBC, EICC

Introduction

The ocean has a profound impact on the earth's climate and thus affects all forms of life on earth. Especially in some regions, the wind and ocean current's regime control the lives of millions of people. Such is the case for India and the Monsoons. The term 'Monsoon' describes the seasonal changes in atmospheric circulation and precipitation. Winds that blow over the Indian Ocean are the main forcing function and reverse twice during the year. They blow from southwest during May-September and from northeast during November-February. The inbetween months are the transition months. These changes have both positive and negative effects on India's population. They either contribute to society and economy by creating a surplus of crops or cause damages by destroying properties and taking the lives of thousands of people.

Understanding, describing and showing ocean circulation remains a challenge. Despite the progress made it remains difficult to build a singular ocean model so robust that it can display accurately the phenomena all over the world. Nevertheless, most of the existing models have proven to be succesful in depicting most of the parts of the ocean and to be consistent with available hydrographic and remotley sensed observations. Some of the models used in oceanography studies are POM (The Princeton Ocean Model), SYMPHONIE and ROMS (Regional Oceanic Modeling System). The latter is an approach to regional and basin-scale ocean modeling available for free on the internet (www.romsagrif.org) and the one that has been used in this study in order to model the circulation regime in the Bay of Bengal.

The application of the model is coupled with the specific characteristics of the region chosen. Thus the current pattern, the temperature and the salinity of the bay can be diagnosed. First the model is described and then its results are presented. Finally the outputs of the ROMS model are compared to the results of an Ocean General Circulation Model applied by Vinayachandran et al. (1996), to a high resolution three layer non-linear model applied by Hacker et al.(1998) and finally to an isopycnic layered model used by Potemra et al. (1991).

Materials and Methods

Study Area

The Bay of Bengal is located in the northeastern part of the Indian Ocean ($\sim 6^{\circ}$ to 22° N and 80° to 94° E) and it is the largest bay in the world (surface area : $\sim 2 \times 10^6$ km 2). To the north it is bordered by Bangladesh, to the east by Myanmar and to the west by India and the island of Sri Lanka. The Andaman and Nicobar Islands along the eastern boundary separate the bay from the adjacent Andaman Sea. The Bay of Bengal annualy receives large amounts of freshwater through river discharges and heavy precipitations especially during the summer monsoon season (estimated inputs over 200 km 3). Some of it's major rivers include the Ganges, the Brahmaputra, the Krishna and the river Mahanadi. This water produces a warm, low-salinity and high nutrient and oxygen-rich water layer to a depth of 100 m that stretches over a distance of 1 500 km.



Fig1. The bay of Bengal, the Andaman Sea, the Malacca Strait between Indonesia and Malaysia.

Ocean Models Presentation

The observations made from satellites are restricted to the surface and those made by boats and drifters are sparse. The arrival of numerical models inaugurates an era of a more holistic view of the ocean currents. These models overcome the existing problems when it comes to the solution of the equations of motion for example. These equations, representing oceanic flows, are impossible to be solved analytically due to the non-linear terms of turbulence. The arrival of more powerful computers, coupled with a more extensive ocean surveillance (i.e. satellite altimetry), have extended the area and period of observation but models can never give a complete description of the global circulation pattern. As Stewart (2008) explains this problem arises from various sources; the nature of the equations (the motion of the ocean is demonstrated by differential equations while numerical models use algebraic approximations), the difficulty of calculating the turbulence, the oversimplification of the oceanographic models and the factor of software errors (bugs).

Simulation models calculate realistic oceanic circulation by resolving the primitive equations coupled with the international equation of state of seawater, as well as the equations of temperature and salt conservation. The approximations are based on several hypothesis. First of all, under the hydrostatic approximation it is assumed that the vertical gradient of pressure is balanced with the buoyancy force. This is based on the fact that the horizontal dimensions of the ocean are more important than the vertical dimensions. Allowing us to consider the ocean as shallow waters, a first simplification of the Navier-Stokes equation on the vertical can be achieved. Furthermore we consider seawater as an incompressible fluid, which is equivalent to the Boussinesq approximation that assumes density is relatively constant in space and time except when it is multiplied by the gravity acceleration in calculations of pressure. This assumption simplifies the continuity equation.

$$\begin{aligned}
 (1) \text{ Hydrostatic equation} \quad 0 &= -\frac{\partial P}{\partial z} - \rho g \\
 (2) \text{ Continuity equation} \quad 0 &= \frac{\partial u}{\partial x} + \frac{\partial v}{\partial y} + \frac{\partial w}{\partial z}
 \end{aligned}$$

Because of the high complexity of the turbulent's terms, Reynolds proposed to split the variables of velocity and pressure into a mean and a fluctuating part $u = \bar{u} + u'$, where the overbar denotes the average and $\bar{u}' = 0$.

$$\begin{array}{lll}
 \overline{u' u'} = -A_x \frac{\partial \bar{u}}{\partial x} ; & \overline{u' v'} = -A_y \frac{\partial \bar{u}}{\partial y} ; & \overline{u' w'} = -A_z \frac{\partial \bar{u}}{\partial z} ; \\
 \overline{v' u'} = -A_x \frac{\partial \bar{v}}{\partial x} ; & \overline{v' v'} = -A_y \frac{\partial \bar{v}}{\partial y} ; & \overline{v' w'} = -A_z \frac{\partial \bar{v}}{\partial z} .
 \end{array}$$

Hence we obtain the equations of conservation of momentum (4a) and (4b) where $A_h = A_x + A_y$,

$$\begin{aligned}
 \frac{\partial \bar{u}}{\partial t} + u \frac{\partial \bar{u}}{\partial x} + v \frac{\partial \bar{u}}{\partial y} + w \frac{\partial \bar{u}}{\partial z} &= -\frac{1}{\rho_0} \frac{\partial P}{\partial x} + f v + A_h \left(\frac{\partial^2 \bar{u}}{\partial x^2} + \frac{\partial^2 \bar{u}}{\partial y^2} \right) + A_z \frac{\partial^2 \bar{u}}{\partial z^2} \\
 \frac{\partial \bar{v}}{\partial t} + u \frac{\partial \bar{v}}{\partial x} + v \frac{\partial \bar{v}}{\partial y} + w \frac{\partial \bar{v}}{\partial z} &= -\frac{1}{\rho_0} \frac{\partial P}{\partial y} - f u + A_h \left(\frac{\partial^2 \bar{v}}{\partial x^2} + \frac{\partial^2 \bar{v}}{\partial y^2} \right) + A_z \frac{\partial^2 \bar{v}}{\partial z^2}
 \end{aligned}$$

and

(5) Conservation of temperature

$$\frac{\partial T}{\partial t} + U \cdot \nabla T = K_h \nabla_h^2 T + K_v \frac{\partial^2 T}{\partial z^2}$$

(6) Conservation of salt

$$\frac{\partial S}{\partial t} + U \cdot \nabla S = K_h \nabla_h^2 S + K_v \frac{\partial^2 S}{\partial z^2}$$

(7) State equation

$$\rho = (T, S, p)$$

The first term of the equation of conversation of momentum (4a and 4b) represents the local acceleration, for the east and west orientated components of velocity. The next three are those related to advection, followed by the gradient of pressure and the Coriolis force that reflects the earth's rotation. The last terms represent the turbulent viscosity.

The outputs of a model differ according to the approach chosen in calculating the coefficients of viscosity (A_h, A_z, K_h, K_z). Different regional models, POM, SYMPHONIE and ROMS, use different hypothesis regarding the horizontal and vertical coefficients of viscosity. First of all the hypothesis of a horizontal isotropic movement is made. The mixing is equal in both directions and depends only on the shear of velocity and on the size of the grid (Smagorinski, 1963). The fundamental problem of "closure", when it comes to studies of turbulent flows, remains unsolved and this is the point were the regional models differ the most. Among several approaches, trying to model the vertical mixing in the water column, those of the Kinetic Energy (Mellor & Yamada, 1974, Gaspard et al., 1990) and the K-profil parametrization (Pacanowski & Philander 1981, Large et al. 1994).

| | ROMS | POM | SYMPHONIE |
|----------------|---|----------------------|---------------------|
| Kinetic Energy | Mellor & Yamada 1974 | Mellor & Yamada 1974 | Gaspard et al. 1990 |
| K-profil | Pacanowski & Philander 1981, Large et al. 1994 | | |

According to Gaspard et al (1990) the vertical turbulent diffusion coefficient of temperature and salt depends on the mixing length and interferes in the equation of turbulence energy created by the shear of velocity. In order to obtain the value of the coefficient, the prognostic equation of the kinetic turbulent energy should be solved and the mixing layer should be estimated. Whereas in the case of Mellor & Yamada (1974) the mixing length is calculated by a different equation. However, when the water column is stratified ($\rho = \text{cst}$) the vertical turbulent mixing is under-estimated. Pacanowski & Philander (1981) and Large et al. (1994) on the other hand, propose a non-local, vertical profile of the coefficients of the turbulent viscosity and diffusion.

ROMS Model

ROMS is a regional, three-dimensional, free-surface, terrain-following numerical model that solves the Reynolds-averaged Navier-Stokes equations using the hydrostatic and Boussinesq assumptions. The model follows a basic principle, as do all ocean models. If the ocean initial state (velocity, temperature etc) is known at a specific given time, along with the boundary conditions of the surface, bottom and lateral sides, then the ocean state at a subsequent time can be calculated. This is possible by using numerical approximations of the primitive equations and by discretizing the equations in time and space.

The boundary conditions are :

Surface boundary conditions ($z = n$)

(8) Kinematic

$$\frac{\partial \eta}{\partial t} = w$$

(9) Wind stress

$$A_v \frac{\partial u}{\partial z} = \tau_{s_x}$$

$$A_v \frac{\partial v}{\partial z} = \tau_{s_y}$$

(10) Heat flux

$$K_v \frac{\partial T}{\partial z} = \frac{Q}{\rho_0 C_p}$$

(11) Salt flux

$$K_v \frac{\partial S}{\partial z} = \frac{S(E - P)}{\rho_0}$$

Bottom boundary conditions ($z = -H$)

(12) Kinematic

$$w = -u \cdot \nabla H$$

(13) Bottom friction

$$A_v \frac{\partial u}{\partial z} = \tau_{b_x}$$

$$A_v \frac{\partial v}{\partial z} = \tau_{b_y}$$

(14) Bottom flux-heat

$$K_v \frac{\partial T}{\partial z} = 0$$

(15) Bottom flux-salt

$$K_v \frac{\partial S}{\partial z} = 0$$

The unkowns of these equations are the prognostic variables u , v , T , S , η (the vertical displacement of the free surface), the diagnostic variables w , P , ρ and the parameters A_v , K_v . The generating force of currents is the wind and the velocity of a current is proportional to the wind stress (equation 9). Surface boundary conditions for salinity are given by the evaporation-precipitation balance (equation 10). No significant exchange of temperature and salt takes place between the sea floor and the sea as groundwater and hydrothermal vents are neglected (equations 14 15).

ROMS model allows to choose between different approches regarding the “closure” of turbulence. Either the Mellon & Yamada (1974) approach or the Pacanowski & Philander (1981)- Large et al. (1994).

After defining the boundary conditions the equations are discretized. In ROMS Model the mode-splitting error is reduced as it is designed with a finite-volume, finite-time-step discretization for the equations. As a result the model is more stable, robust and efficient (Shchepetkin & McWilliams, 2004). For the spatial derivatives, the numerical discretization for a complex topography uses terrain-following curvilinear coordinates in order to better define the coastline. The ROMS horizontal grid is an Arakawa C-grid (Fig. 2) that separates the evaluation of vector quantities (e.g. evaluation of u and v at different centers of the grid). The topography-following vertical grid uses σ -coordinates, $z = z(x, y, \sigma)$ where z is the Cartesian height and σ the vertical distance from the surface, $-1 \leq \sigma \leq 0$, $\sigma = 0$ corresponds to the free surface, $z = \zeta$, and $\sigma = -1$ corresponds to the oceanic bottom, $z = -h(x, y)$. The expression of z may be combined with non-linear stretching $S(\sigma)$ and then obtain $z(x, y, \sigma) = S(\sigma) h(x, y)$ and thus the σ -coordinate is generalized into the S-coordinate (Song & Haidvogel, 1994) which results in a better resolution for shallow waters and regions near the seafloor (Fig. 3).

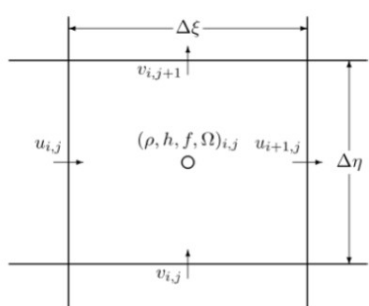


Fig 2. Placement of variables on an Arakawa C

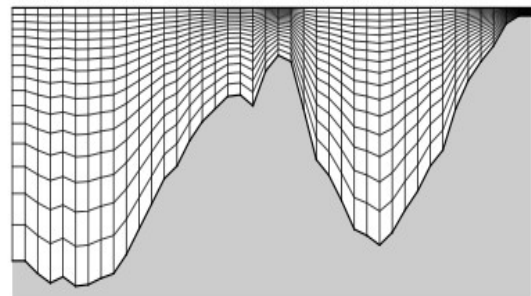


Fig 3. Example of vertical coordinate system, S- coordinate system of Song and Haidvogel, 1994 (Fig. extarcted by Shchepetkin and McWilliams, 2004)

In oceanic modeling the time step is restricted by the internal and the external gravity waves and therefore a coupled barotropic-baroclinic system that separates the time steps (Mode splitting) is recommended. The calculations of the barotropic 2D (shallow water equation) loop are the fastest whereas the baroclinic 3D (primitive-Boussinesq approximated equation) are the slowest but most accurate. The 2D model outputs are time-averaged inbetween the 3D time-steps and at the end their profiles must be coherent. The time step for the internal 3D model is dt and for the external 2D model NDTFAST, these are linked in $dt/NTDFAST = \Delta t_{2D}$. In order to assure the model's stability the Courant-Friedrichs-Lowy criterion is applied. The CFL implies that the time step must respect the equation $\Delta t \leq 1/C |1/\delta x^2 + 1/\delta y^2|^{-1/2}$ otherwise the simulation will produce incorrect results (aliasing). The calculation speed must be superior to the celerity of the propagating gravity waves $\Delta x/\Delta t \geq (gh)^{1/2}$, h being the depth.

Implementation

The first step in building a configuration is to download and decompress the following files: Roms_Agrif_v2.1 that provides the fortran code and ROMSTOOLS that provides the matlab routines to pre-process the input file and to visualize them. Afterwards, we have to verify that the jobcomp script is executable and compile the model code. The executable file roms is then produced. Supplementary files are needed: ad_tools.tar.gz can be downloaded from the internet site <http://www.com.univ-mrs.fr/~doglioli/OPB205/>. Executing start.m allows us to obtain netcdf routines that may not be already included in our Matlab version. Matlab 2007a uses the mexcdf software to access and read the NetCDF libraries. In order to find the coordinates of our specific studying domain we use the ad_findcoord.m script and then modify the coordinates in the param.m script along with the grid longitude resolution (in degrees) and the open boundaries. Now we launch make_grid.m and we obtain the grid, the grid parameters (Table 1) and the bathymetric map (Fig. 4). The grid parameters that will be used for calculating the CFL criteria are saved in a memo.mat file. Since the grid is ready the climatological forcings should be given. The script make_forcing.m provides the atmospheric forcing ,wind stress, surface heat and freshwater flux. The make_clim.m script then provides the lateral oceanic boundary conditions,T,S, SSH, currents. The model is forced with wind stress derived from the International Comprehensive Ocean-Atmosphere Data Project (COADS05).The internal and external time step of the simulation based on the CFL criteria is calculated by the scripts ad_cfla.m. Since $dt = 2400$ s and $NDTFAST = 60$ s, $\Delta t = dt/NDTFAST = 40$ s. The CFL criteria is well respected since $\Delta x/\Delta t = 25000\text{m}/40\text{s} = 625\text{ m/s} \geq (gh)^{1/2} = (9.81 \times 4100)^{1/2} = 200\text{ m/s}$. Note that $1/4^\circ = 25\text{ km}$.

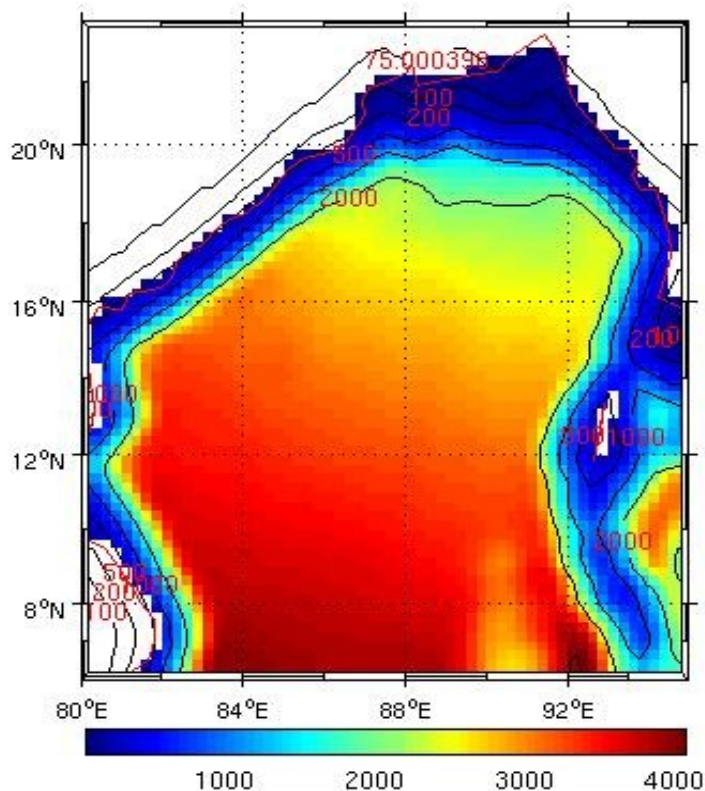


Fig 4. Bathymetry of the Bay of Bengal

| | | | | | | |
|-------------------------------------|----------------------------|---|---------------------------------|--|--|-----------------------------|
| Longitude maximum 95° E | Longitude minimum 80° E | Latitude maximum 23° N | Latitude minimum 6° N | Llm=L-1= 59 L=number of horizontal mesh (x) | Mmm=M-1= 70 M=number of horizontal mesh (y) | hmax (m) 4057,3502= 4100 |
| Open boundaries East,West, South | Grid resolution 1/4° | Vertical grid parameters θs =8 θb=0 | Number of vertical levels 32 | dxmin= 25,552 km | dxmax= 27,631 km | dymin= 25,617 km |

Table 1. Studying area coordinates after launching `ad_findecoord.m` and grid parameters as obtained after launching `make_grid.m`

Furthermore in order to set up the model for our studying area the scripts `param.h` and `cppdefs.h` need to be edited. On the `param.h` we modified the number of grids and in the `cppdefs.h` we verified the open boundaries. The simulation is ready to be launched after verifying that the variables `dt` and `NDTFAST` are in agreement with the CFL criteria. The duration of the simulation for one month is 1080 s. Therefore the snapshot and the average outputs of the model are saved for every three days, `NWRT`=108 and `NAVG`=108 respectively. In the `cppdefs.h` (line 100) it is possible to choose between the different vertical parametrizations proposed by the model. For this study we used the KPP parametrization (define `LMD_MIXING`) and the horizontal coefficient of viscosity by Smagorinski (1963). The model is compiled with `./jobcomp`. It's launched for one year with `./roms roms.in` and for a long simulation we use `qsub qsub_run_roms.sh` after modifying the scripts `roms_inter.in` and `run_roms.csh`. The results are visualised with `roms_gui.m`. Finally the stability of the model can be diagnosed and visualised using `roms_diags.m` and `plot_diags.m` scripts (Fig. 5). Since the initial conditions for density, fluxes of momentum and heat through the sea surface, and the equations of motion are not all consistent the model needs some time to equilibrate, this period of time is called spin-up. The model is more stable when the fluctuations of the variables (black line) are approaching the mean values (red line). Salt is difficult to be modelled so stability is also difficult to be achieved. The results can be exploited from the fifth year of simulation when the kinetic energy seems to stabilise.

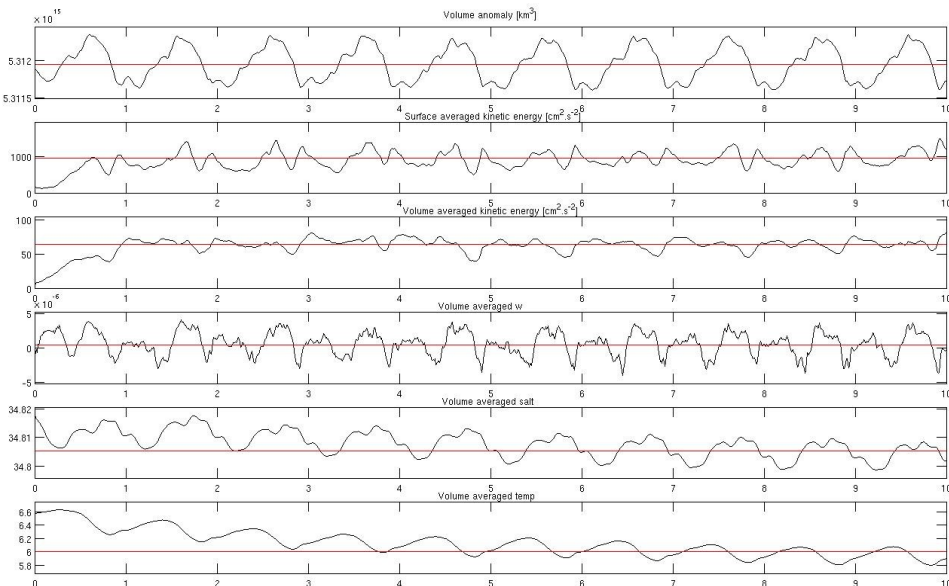


Fig.5 Model's diagnostic (volume and surface averaged quantities) as obtained by `roms_diags.m` and plotted by `plot_diags.m`

Results and Discussion

Wind Circulation

The model clearly depicts the annual wind circulation that alters twice a year (Fig. 6). The wind circulation in the Bay of Bengal is characterized by northeast winds that blow from November to February (day 15 of the simulation) with minimum intensity along the coast and southwest winds that blow from May to September with maximum intensity in the center of the Bay (day 195). The inbetween months are the transition months from winter to the summer monsoon period (day 105) and from the summer to the winter monsoon period (day 285).

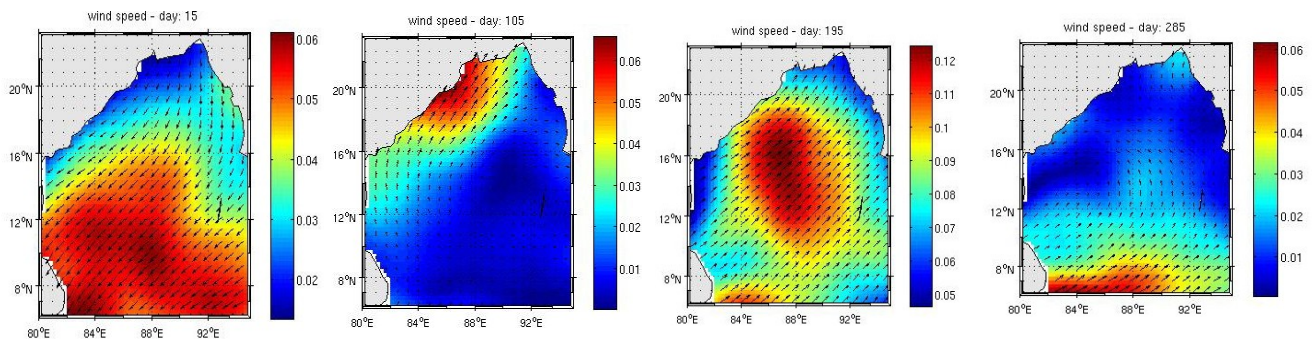


Fig 6. The changing patterns of the wind circulation of the Bay of Bengal obtained by make_forcing.m, day15 : Winter monsoon, day 105 : transition period, day 195: Summer monsoon, day 285: transition period

Temperature and Salt

The seasonal variations of temperature and salinity have been reproduced by the model. The salinity in the Bay is significantly lower in comparison to the Arabian Sea and to the rest of the Indian Ocean. The freshwater discharged from rivers and rainfalls is very important, especially during the summer monsoon (Fig. 7). The fresh plume along the north west part of the Bay is well reproduced by the model even if the river discharge was not included in the model. It does not advect towards the interior of the Bay, not until the end of the southwest winds (Fig. 8). The model shows the seasonal cycle of the sea surface temperature (Fig. 9). The winter cooling is clearly depicted with a minimum of 24°C to the north and a maximum of 28°C to the south. A post-monsoon warming phase is coming next with a minimum of 28° C, again to the North, and a maximum of 29° C. During the summer monsoon the maxima and minima points are inversed hence the minimum is situated to the southwest (28°C) and the maximum to the north (29°C). Finally the model shows the persistence of Warm Pool (28°C) from April to October, already previously observed (Murty et al.1998). This warming of the central basin is caused by the trapping of Kelvin waves in the central Bay for many months and it is an ideal ground for the generation of cyclones (Saheb et al., 2009).

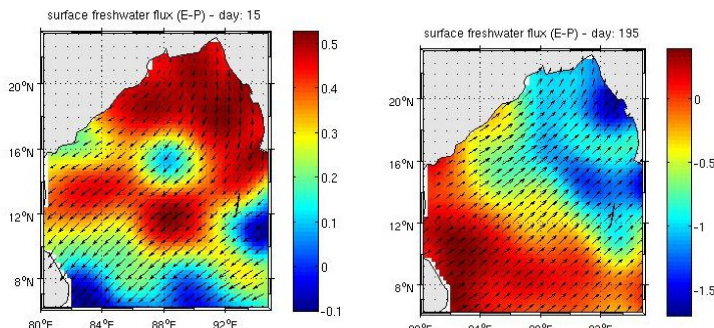


Fig. 7 Surface fresh water flux for day15 : Winter monsoon and day 195: Summer monsoon

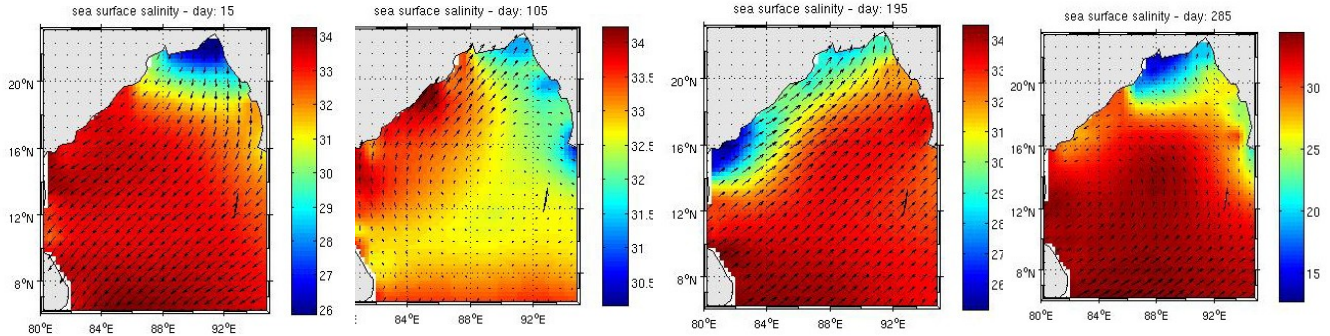


Fig.8 Sea surface salinity of the Bay of Bengal obtained by `make_forcing.m`, day15 : Winter monsoon, day 105 : transition period, day 195: Summer monsoon, day 285: transition period. The fresh plume advects towards the interios of the Bay at the end of the summer monsoon. Note the change of the scale for day 285.

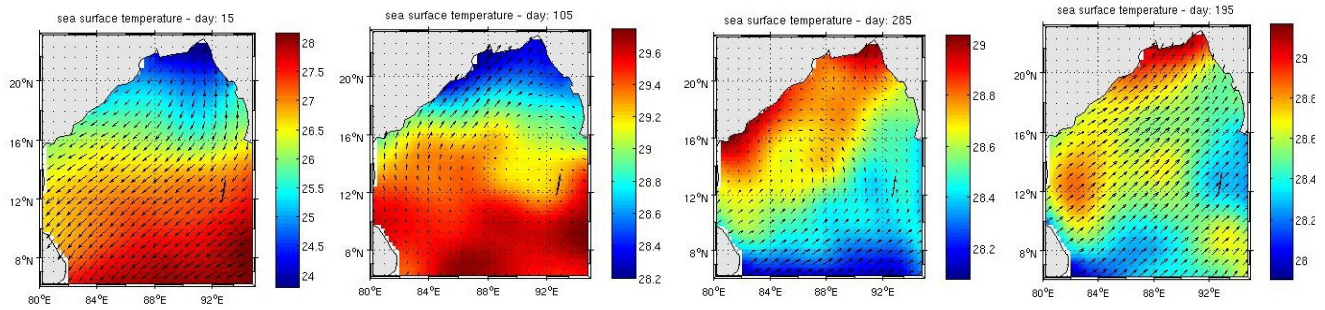


Fig.9 Sea Surface Temperature of the Bay of Bengal obtained by `make_forcing.m`, day15 : Winter, day 105 : Spring, day 195: Summer, day 285: Autumn

General Circulation

The model outputs show a cyclonic gyre that forms in the southwestern Bay of Bengal during October. In December it covers almost the whole bay from 84°E to 93°E and 8°N to 18°N. It dies off until late April where we can only see a cyclonic eddy centered at 12°N 86°E. At the end of June the circulation in the Bay is mainly anticyclonic and dominated by four eddies centered at 10°N 83°E, 11°N 86°E, 15°N 91°E and 8°N 86°E. During July these anticyclonic eddies move towards the west of the Bay and by the end of August the anticyclonic circulation of the Bay is confined to the west of the bay. In September the anticyclonic gyre is much smaller and to the north of the Bay. In November the cyclonic gyre dominates the Bay. It is confined to the west of 93°E longitude and to the south of 20°N latitude and its center waters are cooler than the waters of the surroundings (~2°C), the Bay of Bengal Dome (Vinayachandran & Yamagata, 1998). Another thing is the existence of a southward current, the East India Coastal Current (EICC) (Shetye et al. 1996). This current carries low salinity from the north of the Bay and bifurcates east of Sri Lanka with one major part of it turning towards east and into the Bay (Fig. 10).

During the northeast monsoon and for the first 10 m the model depicts clearly the eddy circulation patterns (Fig. 11a). The cyclonic eddies are centered at 13° N 85° E and 8° N 90° E and the anticyclonic at 11° N 90° E at 17° N 90° E and near the north boundaries of the bay. The model fails to show the anticyclonic gyre (centered at around 92°E 10°N) that dominates in the bay. It is created by the bifurcation of the westward North Equatorial Current (NEC) as it enters the Bay of Bengal from the east of Sri Lanka (Sil & Chakraborty, 2011). The circulation pattern on the subsurface is similar to this of the surface (Fig. 11b). Although we observe a change in direction on the southeast boundaries of the Bay, the entry of the Andaman Sea; northward flow for the surface

layer and southward flow for the subsurface. Two months later, in April, (Fig. 11c) a current along the east coast of India, up to 20°N, is clearly depicted. It can be assumed that it is the western boundary current (WBC) of a seasonal anticyclonic subtropical gyre which forms in the Bay during January, is best developed during March–April, and decays by June (Shetye et al., 1993). This northward current carries warm water from the south and its characteristic feature is the inshore more saline side. The NEC is not capable of producing this western boundary current in the surface during winter probably because of the river discharges (Sil & Chakraborty, 2011). The southward flowing fresh water discharge is opposed to the currents, due to monsoon winds. Furthermore the effects of the strong dominant northeast winds are suppressed in the presence of a strong vertical salinity stratification (Srinivas, 2008). So during winter this boundary current is formed in deeper layers (Fig. 11b) and then appears in the surface during spring (Fig. 12). In addition two cyclonic eddies are shown at 8° N 89°E and at 10° N 84°E and an anticyclonic at 11° N 87°E.

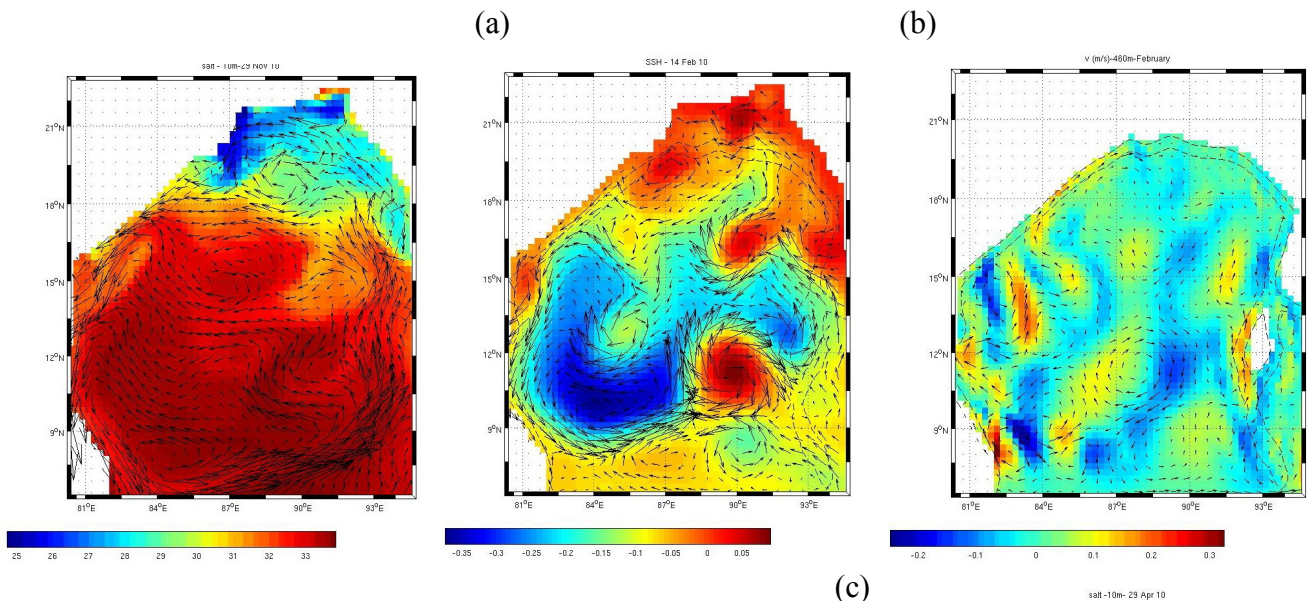


Fig.10 The cyclonic gyre of the Bay of Bengal and the concentration of salt. The low salinity southward EICC is depicted. November, 10m.

Fig.11 Circulation pattern in the Bay of Bengal during (a) February at 10m and (b) at 460 m depth and (c) during April at 10 m. In (a) the sea surface height is illustrated, in (b) the northsouth component of velocity and in (c) the concentration in salt.

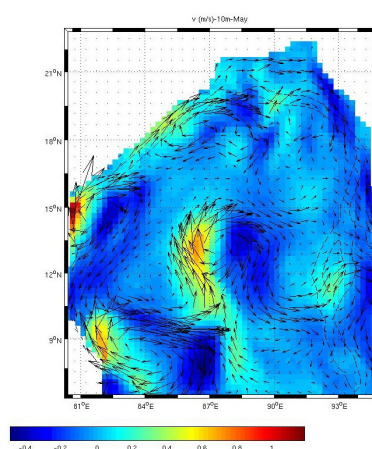
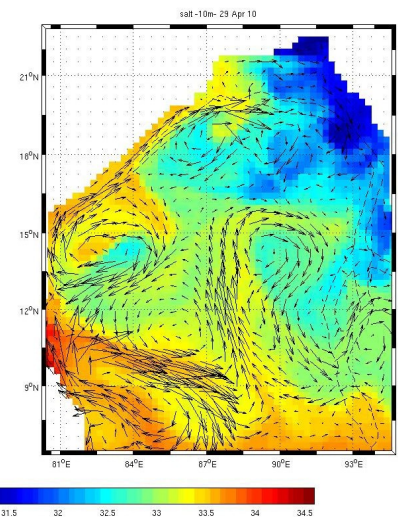


Fig.12 The meridional velocity in the surface for the month of May. The intensification of the anticyclonic eddies along the coast creates the western boundary current (Legeckis, 1987; Johns & Ali, 1992; Somayajulu, 2003; Sil et al., 2010; Sil & Chakraborty, 2011)



The model, for the period of the southwest monsoon, shows that the anticyclonic eddies that were once situated on the north of the Bay (during winter) have now descend towards the south (Fig. 13a). A southward flow on the eastern boundary of the Bay is also visible. The general anticyclonic circulation observed is contrary to the counterclockwise circulation expected (e.g. Potemra et al., 1991). Flow in the next 185 m (Fig. 12b) slightly differs from this on the surface as the southward current on the eastern boundary deviates westward. The area is dominated by two cyclonic and two anticyclonic eddies at 14° N 86° and 15° N 81° E and 11° N 82° E and 14° N 88° E respectively. Another feature of the summer monsoon circulation that the model failed to depict is the coastal current that flows northward in the south and southward in the north (Vinayachandran et al. 1996).

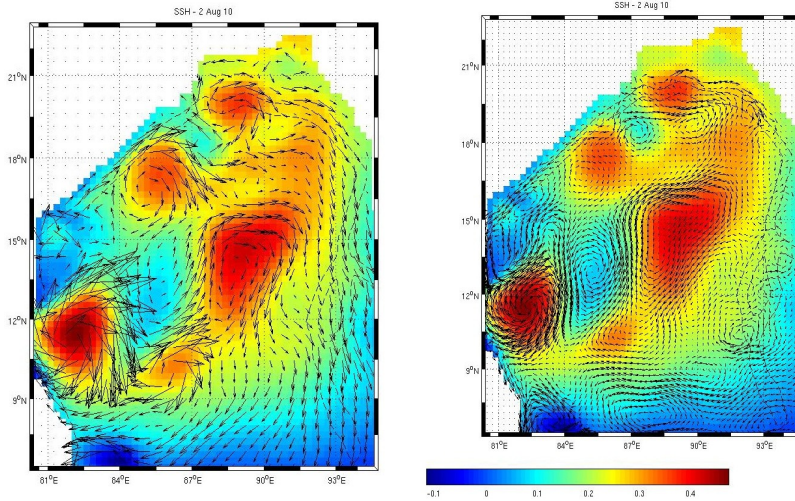


Fig. 12 Circulation pattern in the Bay of Bengal during the southwest monsoon.
(a) 10 m (b) 185 m

In order to evaluate the outputs of the model ROMS for this study, some of the results taken are compared to those from previous studies. We focus on the ability of these models to depict the reversing circulation due to the reversing winds.

In the study of Vinayachandran et al. (1996) of the North Indian Ocean circulation an Ocean General Circulation Model (OGCM) developed by Bryan & Cox (Bryan 1969, Cox 1984) was used. It was forced by climatological monthly mean winds. They chose an unrealistic geometry with a closed southern boundary, no Indonesian throughflow, closed Malacca straight, lack of island chains in the Andaman Sea and smooth bottom topography. They consider that the surface circulation from the 20°S and the Indonesian throughflow has no effect on the circulation of the Bay. Whereas the impact of the closed Malacca Straight and the lack of island chains were unknown. In the surface layer, for February (Fig. 13a) the results from the ship-drifts and their model are coherent. The model shows the anticyclonic gyre and the northward western boundary current that is fed by a northwestward flow in the central Bay and the westward NEC. In our case the circulation simulated by the model fails to clearly depict this pattern and moreover it shows a strong southward flow in the south of the bay. The main reason must be the fact that the north equatorial region is not included in the model and that the Andaman Sea is excluded. Thus the model cannot simulate the westward NEC entering the bay from the Malacca Strait (2° N 102°E), forming eventually an anticyclonic gyre. In August (Fig. 13b), the ship-drifts show an eastward flow in the north of the bay and so does the model of Vinayachandran et al. (1996). Our model also simulates an eastward flow in the north of the Bay. However the northeastward branch of the southwest monsoon current that enters the Bay (Shetye et al. 1996) is not shown by either two models. During May (not shown here), the current along the east coast of India is simulated by our model but not in the Vinayachandran et al. (1996). We should mention that our surface layer is considered at 10 m whereas theirs is at 5 m. Therefore their simulation for 35 m clearly depicts the current along the east coast of India.

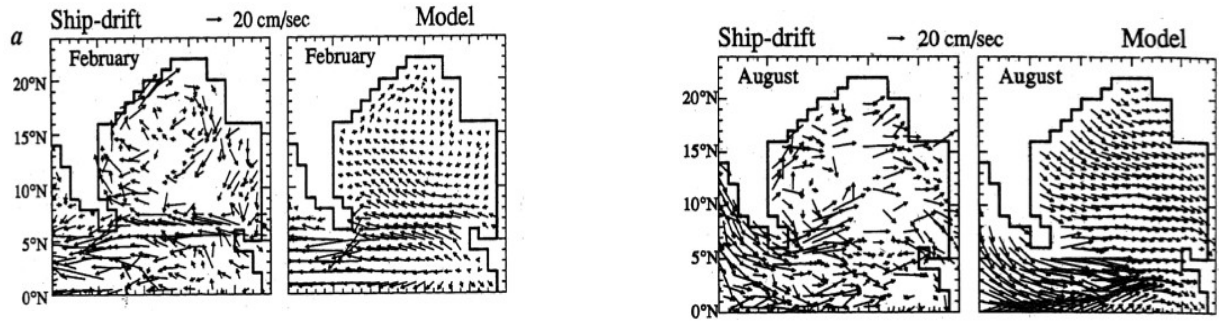
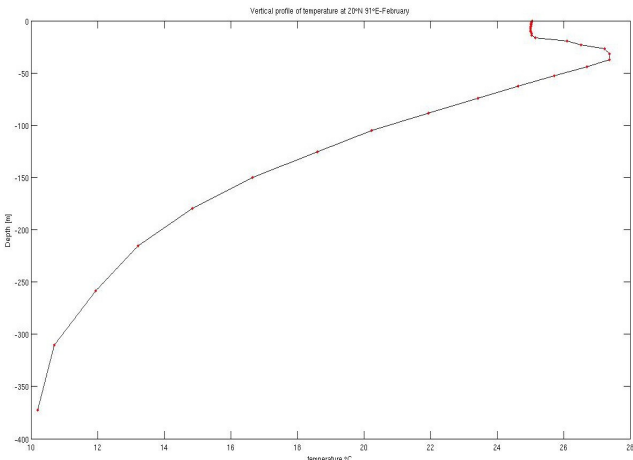
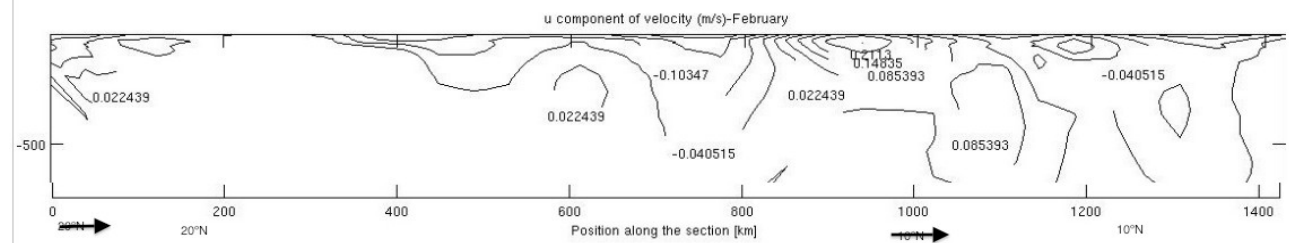


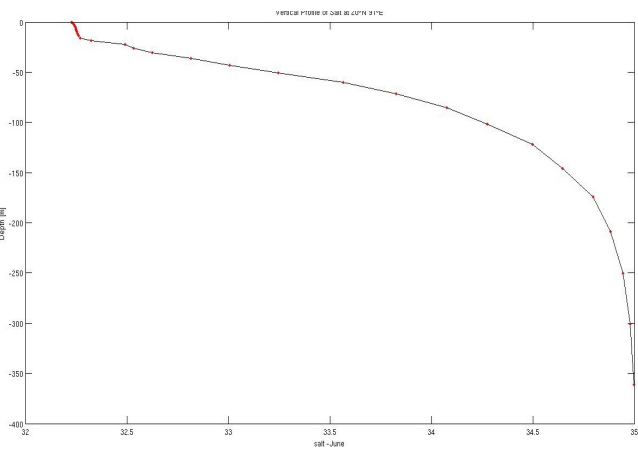
Fig13. Comparaison of the ship-drifts data and the OGCM model outputs applied by Vinayachandran et al. (1996) for the months (a) February and (b) August.

Hacker et al. (1998) made observations of the velocity and the properties of the Bay of Bengal as part of the WOCE (World Ocean Circulation Experiment) during February and March 1995. Afterwards they compared their results to those taken by a high resolution 3 layer non linear model forced by ECMWF (European Center for Medium Range Weather Forecasting) winds. At about 19°N 91°E the ADCP results show a current that flows towards east with a near surface speed over 0.4 m/s (Annex). In the same longitude but at 10° N Hacker et al. observed an eastward flow again of 0.4 m/s and with a high salinity signature of the northwest Indian Ocean. The results of their model were in agreement. Our model also shows eastward flow around 19°N but westward at 10°N. The values of velocity are one order of magnitude smaller (Fig. 14a). The measurements of the temperature from the CTD are in agreement with the outputs of our model. For exemple the vertical profile of temperature for 20°N 91°E (Fig. 14b) shows : A surface maximum of ~28°C and close to 300 m a temperature of ~11°C. The vertical profile of salinity shows surface minimum 32 and a maximum at 35 (Fig. 14c).

(a)



(b)



(c)

Fig14. Vertical profiles of our model outputs (a) zonal velocity at 91°E point 0 km corresponds to 20°N, positive eastward, the contour interval is 0.06 m/s. (b) Temperature at 19°N 91°E and (c) Salinity at 19°N 91°E.

Potemra et al. (1991) applied a multilayer, adiabatic, numerical model to the upper Indian Ocean driven by climatological monthly mean winds. Their model was able to show the interannual patterns of the circulation in the Bay of Bengal such as the anticyclonic flow in the surface waters during the northeast monsoons and its transition to a weaker cyclonic gyre in late summer. The model also showed the intensified western boundary current which changes direction twice a year, according to other authors it is the EICC (Shetye et al. 1996).

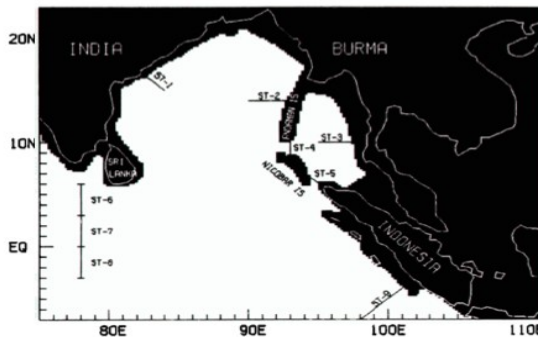


Fig.15 Transect locations after Potemra et al (1991), mass transport in Sv is calculated using the model velocity and the sea surface surelevation data.

In order to quantify this pattern the model calculates the mass transport in selected stations. We also calculated the transport for the two opposite sites ST1 and ST2 (Fig.15) for the month of February and August. According to the results of Potemra et al. (1991) the anticyclonic circulation during winter monsoon is clearly simulated. The values of transport are positive for northward flow and negative for southward flow (Annex). In general the transport on the eastern boundary is weaker than the transport on the western boundary. The ST1 shows a maximum in February (3.5Sv) both for surface and subsurface that indicates the northward flow. For the same month the transport in the eastern station ST2 is negative. The ST1 in August presents once again maximum values of -2Sv (-1.2Sv for the subsurface), but southward this time and ST2 shows positive values. According to our model (Fig. 16a) the surface transport is more important on the western boundary (5 Sv) during winter and on the eastern boundary is negative (-8Sv). In the subsurface (not shown here) the transport is the same as it was on the surface. In August, ST1 has a northward transport (5Sv) and ST2 is around zero (Fig 16b). In the subsurface (not shown here) the transport is once again the same as it was on the surface. Since the choice of the two stations is only approximative and it was not possible to plot a time series of transport these results cannot be considered as reliable. Moreover the circulation in February is not uniform inside the bay. The upper Bay is mainly dominated by anticyclonic eddies whereas further south, a cyclonic circulation is well established. However the comparison of the two components of velocity shows the interannual reversal of currents. For a constant latitude of 18°N the negative surface zonal velocity for February at 85° E, 86°E, 88 ° E and a positive for August shows the change in direction of the circulation patterns (Fig.17). On the other hand Potemra et al. (1991) verifies this alternation but with positive values for February and negative for August. Likewise for the meridional velocity in the subsurface for a constant latitude of 13°N for February, our model gives negative values at 81° E and positive at 92°E. For August the values are both positive. Once again the values of Potemra et al. (1991) oppose ours. Moreover the values obtained by our model are bigger in comparison to Potemra et al. (1991).

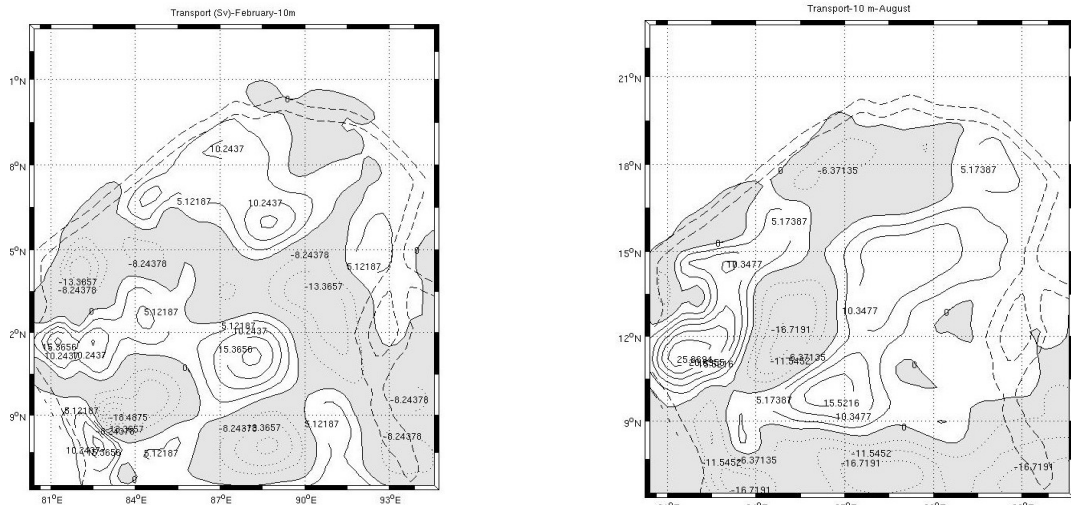


Fig. 16 Transport on the surface Sv for (a) February and (b) August. Positive values imply northward flow whereas negative southward. The contour is 5.

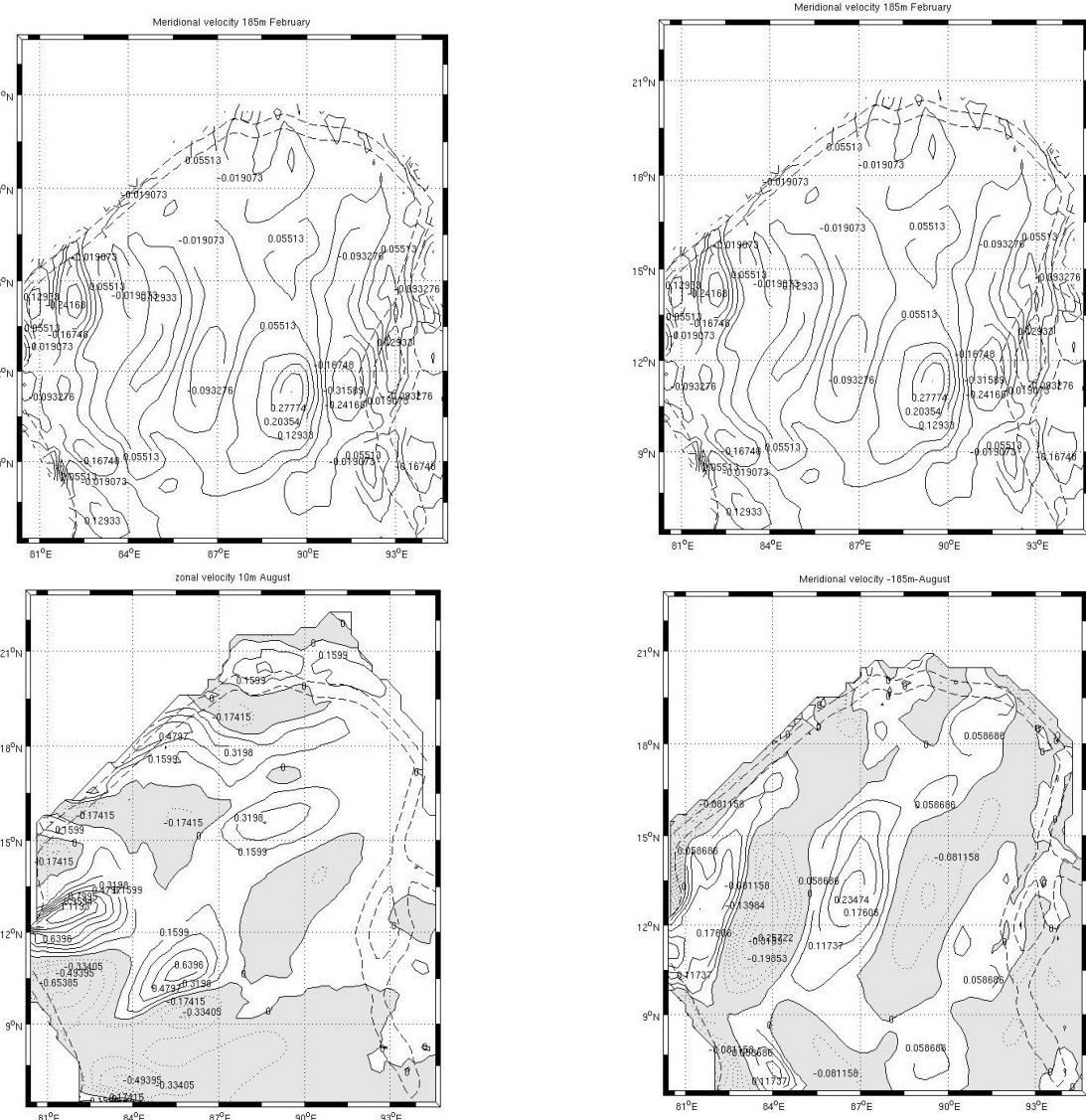


Fig.17 Zonal (surface) et Meridional (subsurface) velocity (m/s) for February (above) and August (below)

Conclusion

The north Indian Ocean and especially the Bay of Bengal have complicated current patterns. The reason for this is the geography of the region and unique wind forces. In order to get an accurate model result, factors such as the freshwater discharge and the equatorial currents must be taken into account. For example the increase in the freshwater southward flow affects the western parts of the Bay by opposing the currents (Srinivas, 1998). Previously studies that implemented a model neglecting freshwater discharge showed an intensification of the premonsoon features. Sea surface salinity was much higher and sea surface temperature was lower (Srinivas & Ram, 2009). Moreover, the Bay of Bengal must be modeled as a whole even to simulate circulation in its parts. Circulation is affected not only by local forces but also from phenomena present outside the region. It was clear in our study that the choice of the grid dimensions were not optimal. For example during the winter monsoon, the westward NEC was not simulated and therefore the characteristic anicyclonic gyre of the Bay of Bengal was not simulated either. Instead a anticyclonic circulation was shown in the north, while a cyclonic was shown in the southwest of the Bay. It was the remaining of the big cyclonic gyre that dominates the premonsoon months. Furthermore the west boundary current was very weak because it was not fed by the NEC and by the general northwestward flow in the center of the Bay. A characteristic feature of the summer monsoon is the coastal current that flows northward in the south and southward in the north, forced by the equatorial winds (Vinayachandran et al.1996). This pattern was not simulated, again probably due to the boundary conditions. The fact that the chain islands of the Andaman Sea were not included in the model is not considered to have a big impact on the results since the resolution that we used was not high enough to clearly “see” them. The Andaman Sea on the other hand should have been concluded as the circulation of the Bay is strongly influenced by the East. The straight between India and Sri Lanka should have been closed too. The model with a $1/4^\circ$ resolution was not able to simulate the flow. Nevertheless the model depicts the seasonal changes especially in the south of the Bay and the mesoescala features that dominate the region. Finally, different models and different conditions produce different simulations. The choice of the right model, its initial and boundary conditions, along with the parametrization chosen for the calculation of either the horizontal or the vertical coefficient of the viscosity can affect the outputs given. In this study a critical comparaison of the particular features of the model mentioned was not made, mainly due to the fact that the results of our model were not reliable.

Bibliography

Bryan K., 1969, J.Comput. Phys., 4, 347-376

Cox M. D., 1984, A Primitive Equation 3-Dimensional Model of the Ocean, GFDL Ocean Group Tech. Rep. No. 1 GFDL/NOAA, Princeton University, Princeton, New Jersey, pp. 141

Hacker P. Firing E. Hummon J., 1998, Bay of Bengal currents during the northeast monsoon, Geophysical Research Letters, Vol.25, 15, 2769-2772

Johns B, Ali A (1992). On the formation of a western boundary current in the Bay of Bengal. J. Marine Syst., 3(3): 267-278.

Large, McWilliams, Doney (1994) Oceanic Vertical Mixing: a Review and a Model with nonlocal k-profil boundary layer parametrization. Reviews Geophysics., 32, 363-403

Legeckis R (1987). Satellite observations of a western boundary current in the Bay of Bengal, J. Geophys. Res., 92: 12974–12978

Mellor, G. L., and T. Yamada, 1982: Development of a turbulence closure model for geophysical fluid problems. Rev. Geophys. Space Phys., 20, 851–875.

Michael, and G. Nampoothiri (1996), Hydrography and circulation in the western Bay of Bengal during the northeast monsoon, J. Geophys. Res., 101(C6), 14,011–14,025, doi:10.1029/95JC0330

Murty, V.S.N., Sarma, Y.V.B., Rao, D.P., Murty, C.S., 1992, Water characteristics, mixing and circulation in the Bay of Bengal during southwest monsoon, J. Mar. Re. Volume 50, Number 2, pp. 207-228(22)

Murty V. S. N. , B. Subrahmanyam, L. V. Gangadhara Rao, G. V. Reddy, (1998), Seasonal variation of sea surface temperature in the Bay of Bengal during 1992 as derived from NOAA-AVHRR SST data, International Journal of Remote Sensing Vol. 19, Iss. 12

Pacanowski R.C. And Philander S.G.H., 1981, J.Phys.Oceanogr., 11, 1443-1451

Potemra, J. T., M. E. Luther, and J. J. O'Brien (1991), The Seasonal Circulation of the Upper Ocean in the Bay of Bengal, J. Geophys. Res., 96(C7), 12,667–12,683, doi:10.1029/91JC01045

Saheb P., Arun C., Pandey P.C., Basu S., Satsangi S.K., Ravichndran M., 2009, Numerical Simulation of Bay of Bengal Circulation Features from Ocean General Circulation Model, Marine Geodesy, Vol. 32, 1, pp.1-18

Schott F.A., McCreary Jr. J.P., (2001), The monsoon circulation of the Indian Ocean, Progr. Oceanogr., Vol 51, Issue 1, p. 1-123

Shankar D., Vinayachandran P.N., Unnikrishnan A.S., Shetye S.R., 2001, The monsoon currents in the north Indian Ocean.

Shchepetkin A. F. and J.C. McWilliams. 2004. The Regional Oceanic Modeling System: A split-explicit, free-surface, topography-following-coordinate ocean model. Ocean Modelling 9: 347–404.

Shetye, S. R., A. D. Gouveia, S. S. C. Shenoi, D. Sundar, G. S. Michael, and G. Nampoothiri (1993), The Western Boundary Current of the Seasonal Subtropical Gyre in the Bay of Bengal, J.

Geophys. Res., 98(C1), 945–954, doi:10.1029/92JC02070.

Shetye, S.R., A.D. Gouveia, D. Shankar, S.S.C. Shenot, P.N. Vinayachandran, D. Sundar, G.S. Michael, and G. Nam-poothiri, Hydrography and circulation in the western Bay of Bengal during the northeast monsoon, J. Geophys. Res., 101, 14011-14025, 1996.

Sil S, Chakraborty A, Ravichandran M (2010). Numerical Simulation of Surface Circulation Features over the Bay of Bengal using Regional Ocean Modeling System. *Adv. GeoSci.* 24:117-130

Sil S, Chakraborty A, Ravichandran M., 2010, Numerical Simulation of Seasonal Variations in circulations of the Bay of Bengal, *J.Ocean.Mar.Sc.*, Vol. 2, 5, pp. 127-135

Smagorinski J., 1963. General circulation experiments with the primitive equations : I. The basic experiment. *Mon. Weather Review* 91, 99-164.

Song Y. and D. B. Haidvogel. A semi-implicit ocean circulation model using a generalized topography-following coordinate system. *J. Comp. Phys.*, 115(1):228–244, 1994.

Srinivas C., Ram P., Josyula L., 2008, Effect of River Discharge on Bay of Bengal Circulation, *Marine Geodesy*, Vol.32, 3, pp.160-168

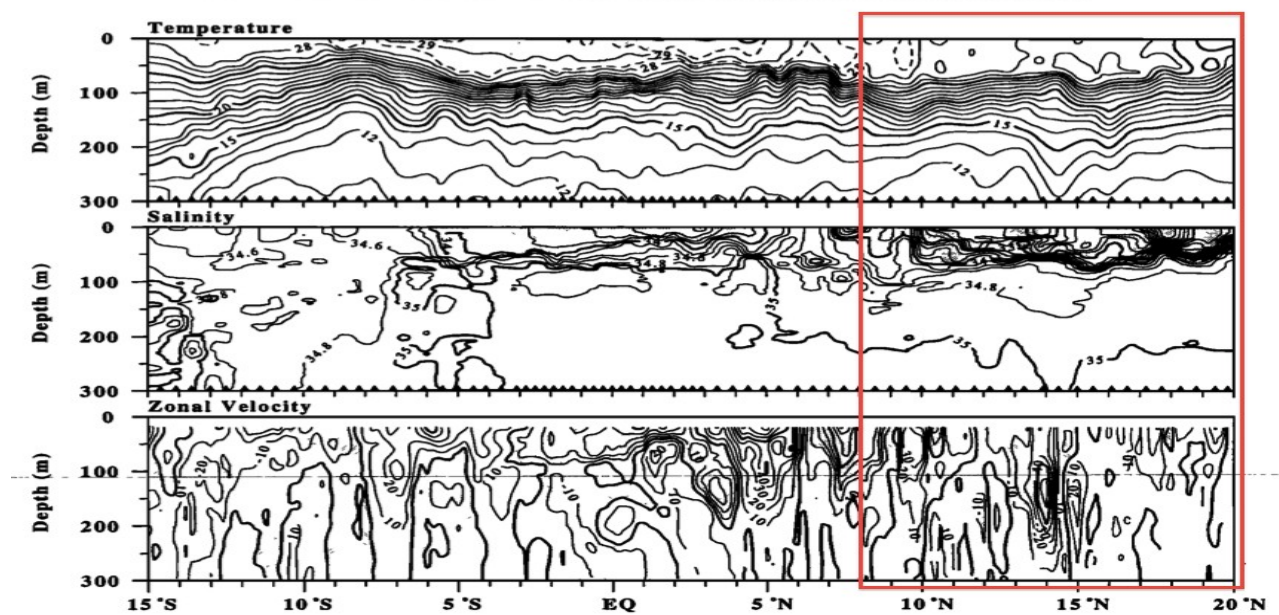
Srinivas C., Ram P., 2009, Role of Fresh Water Discharge from Rivers on Oceanic Features in the Northwestern Bay of Bengal, *Marine Geodesy*, Vol.32, 1, 2009

Stewart R., 2008, *Introduction to Physical Oceanography*, Texas A&M University

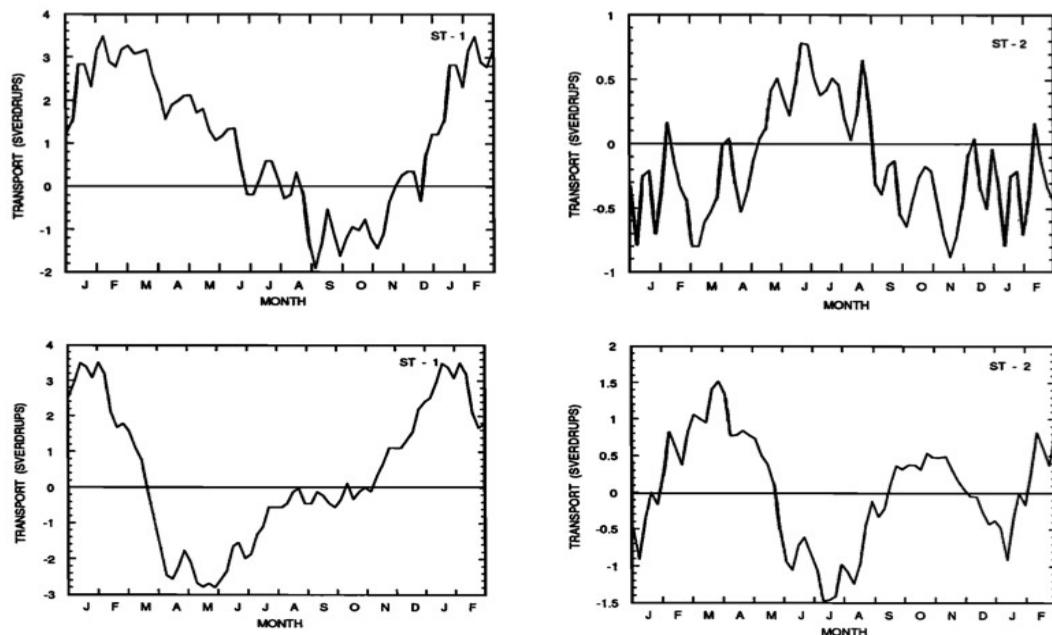
Vinayachandran, PN and Shetye, SR and Sengupta, Debasis and Gadgil, S (1996) Forcing mechanisms of the Bay of Bengal circulation. In: *Current Science*, 71 (10). pp. 753-763.

Vinayachandran, P. N., Yamagata T., 1998: Monsoon Response of the Sea around Sri Lanka: Generation of Thermal Domes and Anticyclonic Vortices. *J. Phys. Oceanogr.*, 28, 1946–1960

Annex



Vertical profiles along the 91°N section of temperature, salinity and zonal velocity, positive eastward, shaded regions are negative and the contour interval is 10 cm/s. ADCP and CTD data collected between February and March 1995, errors in the absolute velocity estimates are less than 0.02 m/s for 1hour averages (Hacker et al.1998).



Time series of mass transport in Sv for ST1 and ST2 displayed as function of days. Positive transport indicates northward flow and negative transport shows southward flow. Surface layer transport is above while the second layer below (Potemra et al.1991).

